Canadian Acoustics / Acoustique Canadienne 19(3) 3-15 (1991) *Research article / Article de recherche*

ISOPARAMETRIC FINITE ELEMENT USING CUBIC HERMITE POLYNOMIALS FOR ACOUSTICS IN DUCT COMPONENTS WITH FLOW

David C. Stredulinsky
Defence Research Establishment Atlantic
P.O Box 1012,Dartmouth, Nova Scotia, Canada, B2Y 3Z7

Anthony Craggs
Department of Mechanical Engineering, University of Alberta
Edmonton, Alberta, Canada, T6G 2J1

ABSTRACT

This paper describes the development of a new finite element model to analyse the propagation of sound through duct system components. The element model was first tested by predicting the acoustic resonant frequencies of hard walled cavities. It was then used to predict the acoustic propagation characteristics of duct bends and junctions, including higher order mode propagation in attached straight ducts, and the convective effect of low Mach number air flow.

SOMMAIRE

Cette communication porte sur la mise au point d'un nouveau modèle à éléments finis d'analyse de la propagation du son dans des éléments d'un réseau de conduites. Les premiers essais du modèle ont consisté à prévoir les fréquences de résonance acoustique de cavités à parois dures. Le modèle a ensuite servi à prévoir les caractéristiques de propagation du son dans des coudes et des raccords de conduites, y compris les caractéristiques de la propagation de mode plus élevé dans des conduites droites raccordées, et l'effet convectif d'un écoulement d'air à faible nombre de Mach.

1 INTRODUCTION

There is a need for improved methods for the prediction of noise transmission and generation in heating, ventilation and air conditioning (HVAC) duct systems. While the propagation of sound waves along a long duct or pipe is quite well understood, the behavior of the sound wave when it is incident on a bend or a junction is not easily calculated without using numerical procedures. At low frequencies (where the wavelength is large compared to the duct width), the sound propagates along a straight duct in a plane wave mode. This plane wave approximation has been used to advantage by Munjal [1] in developing transfer matrix methods for duct and muffler analysis and by Eversman [2] and Craggs and Stredulinsky [3, 4] for the study of branched duct systems.

In Reference [4], exact plane wave solutions are used in straight ducts, and finite element models are employed in components such as bends, duct junctions and plenums where two and three-dimensional propagation effects are important. The finite element models are constrained to plane waves at connecting straight duct interfaces. The procedure was developed on a desktop computer with the aim that it could be used by design engineers on desktop systems. The resulting method was still limited in the size of duct system which could be handled on a "PC" type computer.

As an extension of Reference [4], this paper is concerned with the development of a more efficient acoustical finite element to allow solution of larger problems on a desktop computer. The work is concentrated on propagation through individual duct bends and junctions with a specified incident sound wave entering the bend or junction.

The convective effect of the flow on the sound propagation is considered, but flow generated noise within the duct components is not included. The predictions are extended to higher frequencies by considering higher order mode propagation in connecting straight ducts. The methods developed were implemented on a desktop computer with 1.5 megabytes of RAM, which limited the size of problems that could be solved.

2 THE NEW FINITE ELEMENT

In the earliest work on acoustic finite elements, rectangular brick elements, tetrahedral elements and triangular elements were used. Refer for example to Gladwell [5], Craggs [6, 7], Shuku and Ishihara [8] and Young and Crocker [9]. The edges or surfaces of these elements could only model straight lines or flat planes. A cuboid brick element with Hermite polynomial interpolation functions has been used by several researchers [6, 9, 10] and found to give accurate results and high rates of convergence [11]; however, this element has the disadvantage that it cannot be distorted to model curved boundaries or even oblique flat boundaries. More recently, isoparametric elements which can be distorted to model curved boundaries have been extensively used by Craggs [12], Astley and Eversman [13, 14] and Cabelli [15], for example.

In the present work a new isoparametric element is developed using Hermite polynomials. This new hexahedral element, shown in Figure 1, has thirty-two degrees of freedom and is referred to subsequently as the ISOHERM32 element. Cubic Hermite polynomials are used to approximate the dependent variable functions within the element. These interpolation functions are based on the corner node values of the dependent variable and first partial derivatives. For example, in one dimension, the Hermite polynomial is a cubic function based on the dependent variable and slope at each end of the interval in which it is defined. Additional nodes along the edges of the element (shown in Figure 1b) are used to define the element geometry. For details of the interpolation functions and transformation between the global coordinate system and the local element coordinate system refer to Stredulinsky [16].

In many acoustic problems, typically the acoustic pressure or the acoustic velocity potential is used as the dependent variable. In the initial development of the new element the acoustic pressure was used; however, in later work involving flow, it was found more convenient to use a velocity potential for both the acoustic and flow fields. In the initial development, the four degrees of freedom at each corner of the element were the acoustic pressure P and pressure gradient components $\partial P/\partial x$, $\partial P/\partial y$, and $\partial P/\partial z$. In the later development the velocity potential and velocity potential gradient components were used. The main motivation for using Hermite polynomials in

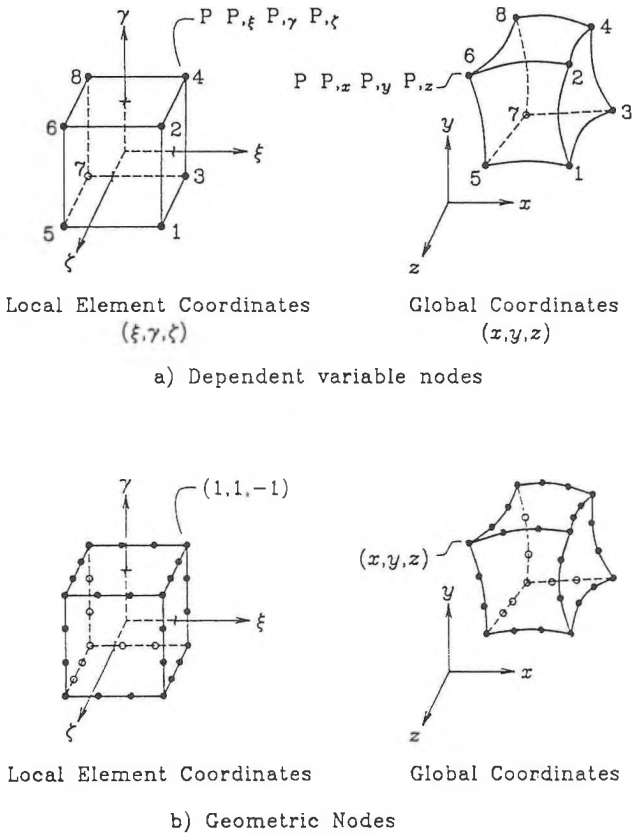

Figure 1: The ISOHERM32 finite element

problems with hard walled ducts is that the gradient degrees of freedom, normal to the duct wall, can be constrained to zero. This leads to smaller global finite element models as discussed in the following paragraph.

The closest "competitive" conventional finite element to the new element is the cubic hexahedral isoparametric element (HEX32), which uses cubic Serendipity interpolation functions. This element also has thirty-two degrees of freedom, given by dependent variables at the eight corner nodes and the two nodes along each edge of the element. The main difference between this element and the new element is that the nodal degrees of freedom of the new ISOHERM32 element are concentrated at the corners of the element. This leads to fewer global degrees of freedom (and thus a smaller system of linear equations to be solved) for models using the new ISOHERM32 element compared to models with the same number of conventional HEX32 elements. For the case of hard walled ducts, with the new element further reductions in the overall global degrees of freedom can be achieved by constraining normal derivative degrees of freedom at the wall to zero (based on the boundary condition of zero normal flow velocity and a zero normal acoustic particle velocity at the hard surface).

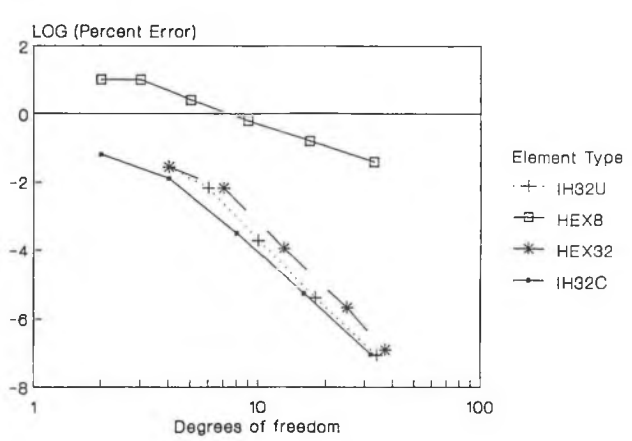

Figure 2: The convergence of different FEM models for the prediction of the natural frequencies for the first axial mode in a 1D tube

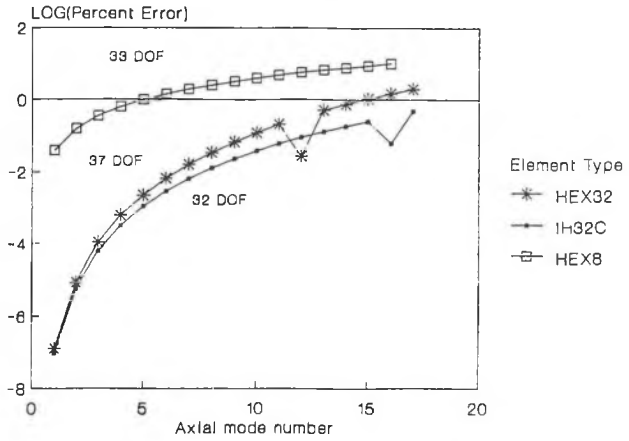

Figure 3: The comparison of different FEM models for the prediction of the natural frequencies of higher order modes in a 1D tube

3 INITIAL TESTING

The new element was initially used to find the acoustic resonant modes and natural frequencies of a stationary compressible fluid within rigid walled cavities for which analytical solutions are known. This problem is governed by the Helmholtz equation which is reduced to a discrete matrix eigenvalue problem using a Galerkin finite element method as described in many textbooks on finite element methods, including Burnett [17].

3.1 A Rectangular Cavity

The solution of the acoustic eigenvalue problem for a rigid walled rectangular cavity is well known, and is given, for example, in Morse [18]. The convergence of the finite element models is demonstrated by considering a linear string composed of one to sixteen cuboid elements with nodal quantities constrained to solve a one-dimensional problem.

The resulting prediction error for the natural frequency of the first axial mode is shown in Figure 2. The $\log_{10}$ of the percent error is plotted as function of the global degrees of freedom for the models. The upper curve, labelled HEX8, for the conventional linear isoparametric element, shows significantly higher errors and a lower rate of convergence than the other three curves which are for the cubic elements. The curve labelled HEX32 is for the conventional 32 degree of freedom hexahedral element. The curves labelled IH32U and IH32C are for the new ISOHERM32 element with the axial acoustic pressure gradient nodal quantities, respectively, left unconstrained (the hard wall boundary condition implicitly satisfied by the finite element method), and explicitly constrained to zero at the rigid ends of the tube. On a number of element bases, the HEX32 model gave slightly better results than the new element, but on a global degree of freedom basis the new element gave more accurate results (typically 1/3 the errors of the HEX32 models).

In Figure 3, the prediction errors for the natural frequencies of higher order axial modes are compared for models with similar numbers of degrees of freedom. The large differences noted between the HEX8 linear element model and the cubic elements for the first axial mode become progressively smaller as the mode number is increased. The ISOHERM32 element curve, labelled IH32C, shows progressively better results than the conventional cubic element HEX32 curve as the mode number is increased. The notches in the graphs for the HEX32 and IH32C curves occurred when each finite element modelled exactly one half wavelength.

The elements used in the above one-dimensional tube problem are undistorted, maintaining the cuboid parent element shape. Figure 4 shows a rigid walled rectangular cavity modelled using two ISOHERM32 elements. The elements are distorted first by rotating the common plane between the elements and then by twisting this plane. The errors in the fifteen resonant frequencies predicted with this model are given in Table 1 for rotation of the common plane and in Table 2 for twisting of this plane. The parameter ka used in these tables and subsequent tables and figures is a non-dimensional frequency parameter based on the wave number k and a typical dimension a taken in this case to be the length of the cavity in the x direction The distortion has the greatest effect on the axial modes along the x axis and very little effect on the axial modes in the y and z directions. The prediction for the first axial mode $[n_x, n_y, n_z] = [1, 0, 0]$ was found to be extremely sensitive to the twisting distortion. Additional results were obtained with the conventional HEX32 isoparametric element. The ISOHERM32 and HEX32

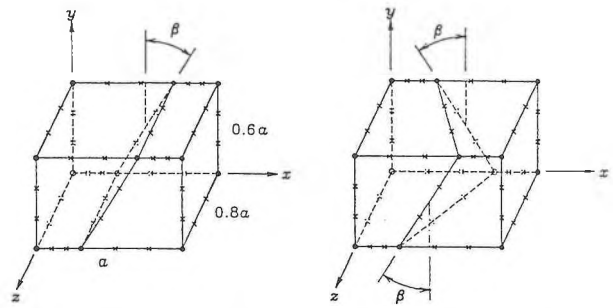

Figure 4: Element distortion within a two-element model of a rectangular cavity

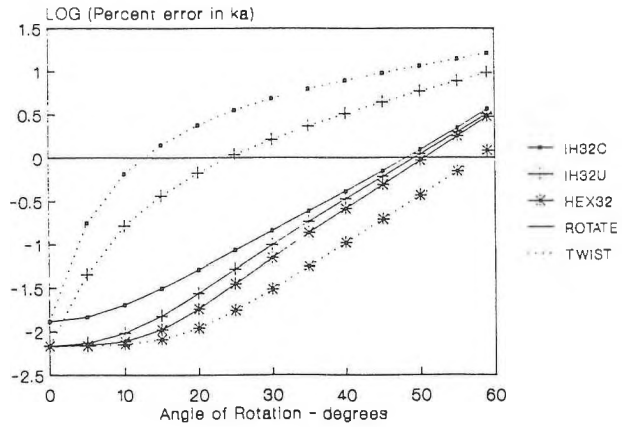

Figure 5: The effect of element distortion on the error in natural frequencies for a two-element model of a rectangular cavity

Table 1: Prediction errors for the natural frequencies of a two-element rectangular cavity with the common plane rotated

Mode				Percent Error in ka				
				Rotation angle in degrees				
No.	n_x	n_y	n_z	0	15	30	45	59
1	1	0	0	0.0130	0.0313	0.1439	0.7071	3.668
2	0	0	1	0.0646	0.0646	0.0646	0.0646	0.0646
3	1	0	1	0.0445	0.0516	0.0955	0.3158	1.486
4	0	1	0	0.0646	0.0639	0.0620	0.0593	0.0573
5	1	1	0	0.0509	0.2975	1.269	4.177	13.49
6	2	0	0	0.0646	0.3444	2.358	10.89	50.15
7	0	1	1	0.0646	0.0641	0.0629	0.0612	0.0599
8	1	1	1	0.0549	0.2294	0.9184	2.991	9.732
9	2	0	1	0.0646	6.2659	1.717	7.958	37.93
11	2	1	0	0.0646	1.333	5.919	17.25	43.86
13	2	1	1	0.0649	1.096	4.847	14.23	36.72
14	3	0	0	3.008	5.305	13.75	37.12	156.4
18	3	0	1	2.578	4.546	11.83	32.29	139.8
20	3	1	0	2.322	5.654	16.16	38.29	124.6
24	3	1	1	2.060	5.014	14.39	34.37	113.8

Table 2: Prediction errors for the natural frequencies of a two-element rectangular cavity with the common plane twisted

Mode				Percent Error in ka				
				Rotation angle in degrees				
No.	n_x	n_y	n_z	0	15	30	45	59
1	1	0	0	0.0130	1.405	4.859	9.572	16.35
2	0	0	1	0.0646	0.0640	0.0627	0.0615	0.0611
3	1	0	1	0.0445	0.6566	2.233	4.942	11.16
4	0	1	0	0.0646	0.0634	0.0608	0.0562	0.0577
5	1	1	0	0.0509	0.7616	2.495	4.987	9.848
6	2	0	0	0.0646	0.3193	1.851	6.685	17.36
7	0	1	1	0.0646	0.0637	0.0631	0.0569	0.0598
8	1	1	1	0.0549	0.7048	2.374	5.898	20.08
9	2	0	1	0.0646	0.1232	1.183	4.754	14.68
11	2	1	0	0.0646	0.1229	1.121	4.293	14.52
13	2	1	1	0.0649	0.8284	3.693	11.55	38.59
14	3	0	0	3.008	3.366	8.658	20.04	38.70
18	3	0	1	2.578	5.560	13.60	28.68	67.79
20	3	1	0	2.322	6.577	18.73	33.97	94.71
24	3	1	1	2.060	4.519	13.78	41.10	122.8

models are compared in Figure 5 where the $\log_{10}$ of the percent error is plotted as a function of the angle of rotation β. Both models show similar behavior for rotation of the common plane; however, the conventional HEX32 model does not exhibit the high sensitivity to twist observed with the new ISOHERM32 element model for the first axial mode. Most of the subsequent work is limited to two-dimensional problems, to reduce the sizes of the computer models, and thus does not involve twisting of element planes. Certainly, further investigation is needed to resolve this problem if general three-dimensional models are to be used.

3.2 A Circular Duct Cross-section

A more realistic problem, involving distortion of the element boundaries, but which still has an analytical solution, is the prediction of natural frequencies of a cylindrical cavity.

This is considered with a two-dimensional version of the new ISOHERM32 element, referred to as ISOHERM12, and the conventional two-dimensional cubic isoparametric element HEX12, using the single-element and four-element models shown in Figure 6. The solid circles at each node represent the acoustic pressure degrees of freedom and the short arrows represent the pressure gradient degrees of freedom. In the constrained models, the arrows represent the effective gradient degrees of freedom after explicitly constraining the normal acoustic pressure gradient to zero at the hard surface. In the lower three models, one edge of each element was collapsed to a point at the centre of the circle.

Table 3 shows the prediction errors in natural frequencies for these finite element models of a circular cross-section of radius a. The first number m in the mode

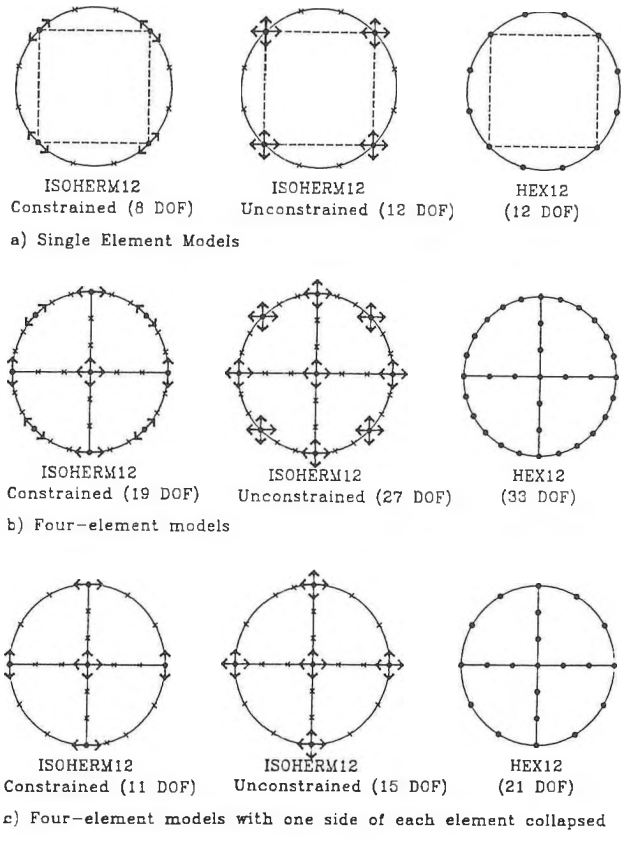

Figure 6: Finite element models of a circular duct cross-section

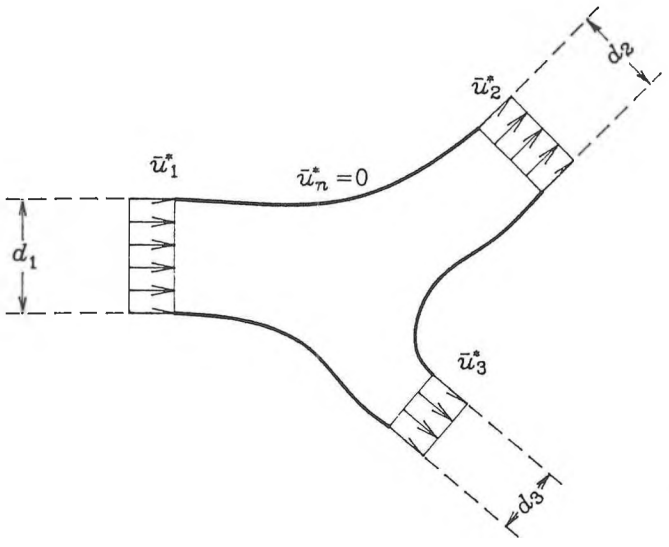

Figure 7: Model of a duct junction showing inlet and outlet flows

description refers to the angular coordinate direction and the second number n to the radial direction. The errors are much higher than obtained when modelling rectangular enclosures with undistorted elements. Of particular interest, the four-element model using the new element, with one collapsed edge and constrained degrees of freedom at the wall, has only 11 degrees of freedom and gives significantly smaller errors than the conventional isoparametric HEX12 single-element model which has 12 degrees of freedom and similar errors to the four-element HEX12 model having 21 degrees of freedom.

4 DUCT COMPONENTS WITH FLOW

Figure 7 shows a general two-dimensional model of a duct junction. The junction region is attached to three infinitely long (or anechoically terminated) straight ducts containing uniform flow at velocities $\bar{u}_1^*$, $\bar{u}_2^*$ and $\bar{u}_3^*$. The incident wave (which could be a combination of several modes) is specified in one of the ducts. The problem is then to determine the flow field and acoustic field in the junction region, and to determine the reflected acoustic modes in the incident wave duct and the transmitted modes in the other connected ducts.

4.1 Model Development with Flow

Acoustic propagation in non-uniform ducts in the presence of mid to high subsonic flows has been considered by Sigman et al [19], Eversman and Astley [14, 20], and Ling et al [21]. Cabelli [15] considered the influence of flow on the acoustic characteristics of a duct bend with inlet Mach numbers in the range of 0.25 to 0.4. Computing the mean flow field alone is a significant problem. In the work referenced above either approximate flow models applicable to specific geometries were used, or numerical solutions to the inviscid compressible potential flow problem were implemented.

Since flow velocities in HVAC systems are generally low (less than Mach 0.1), a flow model similar to that described by Peat [22] has been incorporated in this work. Acoustic wave propagation is a compressible phenomenon, therefore compressible potential flow equations are used as in [19], with the velocity potential, ϕ^*, as the dependent variable. It is acknowledged that an ideal inviscid flow model may not realistically represent the real flow in many cases but should at least give some indication of effect of flow on the acoustic propagation at low Mach number.

Dimensionless quantities, the velocity potential $\phi = \phi^*/(Mc_0a)$, time $t = t^*c_0/a$ and angular frequency $\omega = \omega^*a/c_0$ are defined based on the ambient speed of sound c_0, the typical flow Mach number M, typical dimension a, time t^* and angular frequency ω^*. Note that the dimensionless angular frequency $\omega = ka$ where k is the

Table 3: Natural frequencies for a circular cross-section of a hard walled duct

Model	Element	DOF	Percent Error in ka					
			Mode $[m,n]$					
			[1,0]	[2,0]	[0,1]	[3,0]	[4,0]	[1,1]
1 EL	IH12C	8	8.855	33.57		54.97	52.99	
	IH12U	12	3.548	24.29	154.9	51.48	52.99	196.3
	HEX12	12	2.688	14.11	92.80	33.14	27.76	141.3
4 EL	IH12C	19	0.287	2.926	.168	5.215	2.762	3.447
	IH12U	27	0.200	2.815	.087	3.684	2.642	3.447
	HEX12	33	0.122	2.549	.136	4.174	4.330	5.770
4 EL Collapsed	IH12C	11	0.475	0.500	.769	4.533	6.391	8.259
	IH12U	15	0.437	0.490	.400	4.488	6.387	8.259
	HEX12	21	0.196	2.095	.006	8.071	4.971	12.21
Exact ka			1.841	3.054	3.832	4.201	5.318	5.331

wave number. The total flow velocity potential is split into a steady mean flow potential $\bar{\phi}$ and a small acoustic harmonically fluctuating potential $\phi' e^{\mathbf{i}\omega t}$. With this, and the assumption that the Mach numbers are small, the compressible potential flow equations are reduced to the Laplace equation for an incompressible steady flow

$$\nabla^2 \bar{\phi} = 0, \tag{1}$$

and a second equation involving this mean flow velocity potential and the acoustic velocity potential ϕ' given by

$$\nabla^2 \phi' + \omega^2 \phi' - 2\mathbf{i} M \omega \nabla \bar{\phi} \bullet \nabla \phi' = 0. \tag{2}$$

The steady flow potential can be obtained from Equation 1 and then substituted into Equation 2 to find the acoustic velocity potential. Note that if there is no flow, $\nabla \bar{\phi} = 0$, and Equation 2 reduces to the Helmholtz equation.

A Galerkin finite element procedure is applied with the new element to reduce these differential equations governing the continuous acoustic and flow fields to a system of linear equations in terms of the unknown discrete nodal acoustic and flow velocity potential quantities.

The acoustic boundary conditions at the interfaces of the finite element model of the junction and the connecting straight ducts can be determined based on the analytical solution of governing equations for the case of uniform flow in a straight duct. Alternatively, the better known solutions of the convected wave equation, valid for uniform flow at higher Mach numbers can be adopted; refer for example to Munjal [1, Chapter 1] and Morfey [23]. The differences between the solutions is small for low Mach numbers and both take the form

$$\phi' = \sum_{m=0}^{\infty} \Phi_m(y,z) \left(A_m e^{\mathbf{i}\omega_m^+ x} + B_m e^{\mathbf{i}\omega_m^- x} \right) \tag{3}$$

for a straight duct of arbitrary cross-section, where x is the dimensionless coordinate along the axis of the duct and y and z are in the plane of the duct cross-section. The term $\Phi_m(y,z)$ defines the m^{th} mode shape for the cross-section. The terms ω_m^+ and ω_m^- are a function of the dimensionless angular frequency ω, the flow Mach number and the natural frequency of the m^{th} mode. The modes can be evanescent or propagating depending on whether ω_m^+ and ω_m^- are real or complex quantities.

In linking the straight ducts to the finite element models of a junction or bend, the connecting straight duct acoustic mode shapes and natural frequencies are determined from finite element models of the duct cross-section. This is illustrated for the simplest case of a rectangular duct cross-section modelled with one finite element. The derivative nodal quantities at the hard wall boundaries in the plane of the cross-section can be set to zero leaving four corner nodal velocity potential values to define the modes. In this case the plane wave mode [0,0], and the cross modes [1,0] [0,1] and [1,1] can be approximated as shown in Figure 8. The vector of incident wave nodal velocity potential values can then be written as a modal matrix multiplied by a vector $\{a\}$ defining the incident modal mixture (the mixture of incident plane wave and higher order modes) in one of the connecting ducts. For this simple example the interface nodal acoustic velocity potentials are given by

$$\begin{Bmatrix} \phi'_1 \\ \phi'_2 \\ \phi'_3 \\ \phi'_4 \end{Bmatrix} = \begin{bmatrix} 1 & -1 & 1 & -1 \\ 1 & 1 & 1 & 1 \\ 1 & -1 & -1 & 1 \\ 1 & 1 & -1 & -1 \end{bmatrix} \begin{Bmatrix} a_1 \\ a_2 \\ a_3 \\ a_4 \end{Bmatrix}. \tag{4}$$

Similarly vectors $\{b\}$, $\{c\}$ and $\{d\}$ etc. are defined for

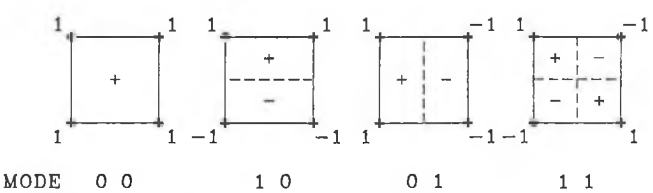

Figure 8: Modes for a rectangular duct cross-section modelled with one element

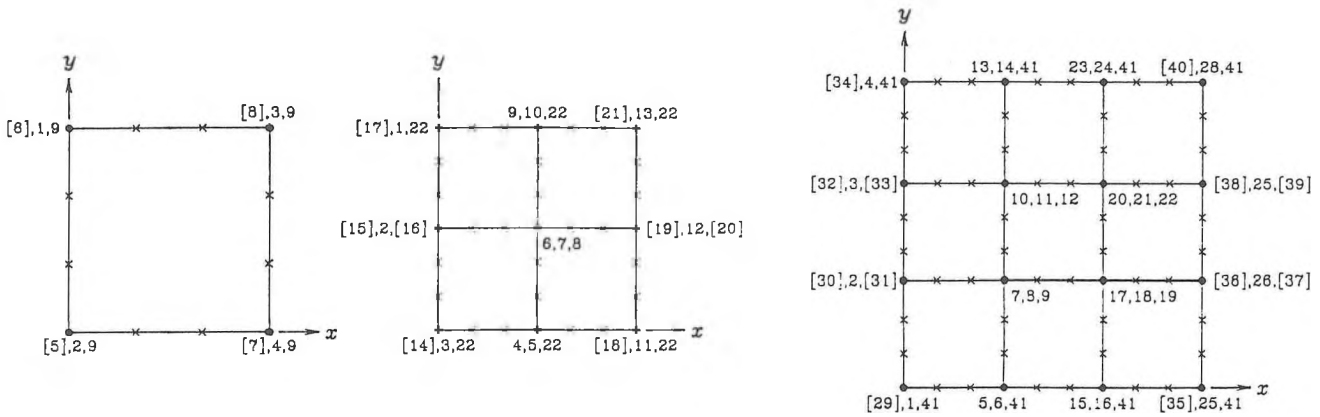

Figure 9: Two-dimensional finite element meshes for models of a straight duct segment

the the reflected modal mixture and transmitted modal mixtures in the remaining ducts.

The derivation and details of the finite element equations are given in reference [16]. Since the finite element model contains no internal source terms, the unknown acoustic velocity potentials and gradient quantities at internal nodes in the model can be eliminated from the resulting linear system of equations, leaving a final matrix equation which is solved for the real and imaginary parts of the unknown transmitted and reflected modal mixtures, given a specified mixture of incident modes.

4.2 Testing the Finite Element Model: A Straight Duct

The finite element model for prediction of acoustic propagation with flow was initially tested for a straight duct of rectangular cross-section. Figure 9 shows two-dimensional finite element meshes for a duct segment of width a in the y direction and of length a in the x direction, with one, two and three elements across the width of the duct. Infinitely long connecting straight ducts are extended to the left and right of the model. The left side of the model has been assigned the incident wave modal mixture and the flow taken as positive from left to right. The global node numbering scheme is shown with a group of three numbers at each node. The first number in each group represents the velocity potential degree of freedom ϕ, and the remaining two respectively, the $\partial\phi/\partial x$ and $\partial\phi/\partial y$ degrees of freedom. In this case the inlet and outlet duct modes are defined in terms of nodal quantities shown in square brackets at each end of the model. The highest node number in each model is assigned to all nodal degrees of freedom explicitly constrained to zero at the hard walls of the duct.

Typical results are shown in Figure 10 for the case of a specified unit incident first cross mode velocity potential. The graphs show the real (RE) and imaginary (IM) parts of the outlet first cross mode acoustic velocity potential, at the lower wall of the duct, for models with one, two and three elements spanning the duct cross-section. The analytical solution is shown by the solid line. The left graph is for a flow at Mach number $M = 0.1$ in the same direction as the acoustic propagation. The right graph is for the case of the flow in the opposite direction. The cut-on frequency for this mode occurs in this case at $ka = 0.995\pi$ (when the duct width is close to half a wavelength). Below the cut-on frequency the mode is evanescent and decays between the inlet and outlet, but above this frequency the mode propagates unattenuated. The prediction errors increase as the non-dimensional frequency parameter ka increases. The results converge closer to the exact solution as the mesh is refined. Also the predictions with flow in the opposite direction to the acoustic propagation show greater errors than that for propagation in the same direction as the flow.

4.3 Modelling a 90° Bend

Figure 11 shows example finite element meshes used to model a duct bend with an inner corner radius equal to half the duct width. The predictions obtained with these models are given in Figure 12 and compared to results obtained by Cabelli [15] using a conventional isoparametric finite element model. The graph shows the velocity potential transmission coefficient $T_{\phi'}$ for the transmitted plane wave and first cross mode components and the reflection coefficient $R_{\phi'}$ for the reflected plane wave and first cross mode. Three elements were needed across the duct width for the predictions to converge to Cabelli's result over the frequency range considered. Below the cut-on frequency of the first cross mode in the connecting ducts, only the plane wave mode is reflected and transmitted. At low frequencies most of the acoustic energy is transmitted; however, as the cut-on frequency of the first cross mode is approached most of the sound energy

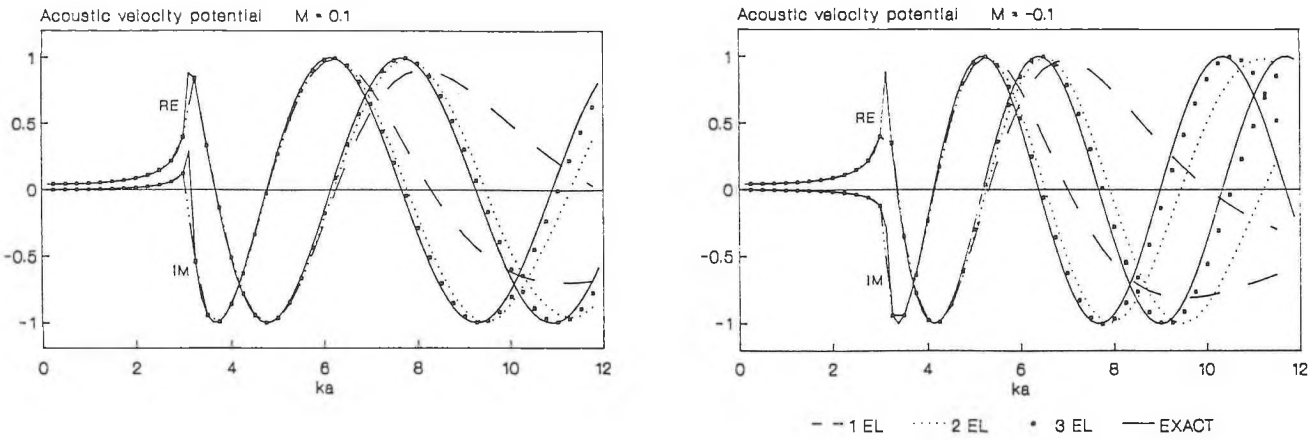

Figure 10: Outlet acoustic velocity potential for the first cross mode in a straight duct segment of width a and length a

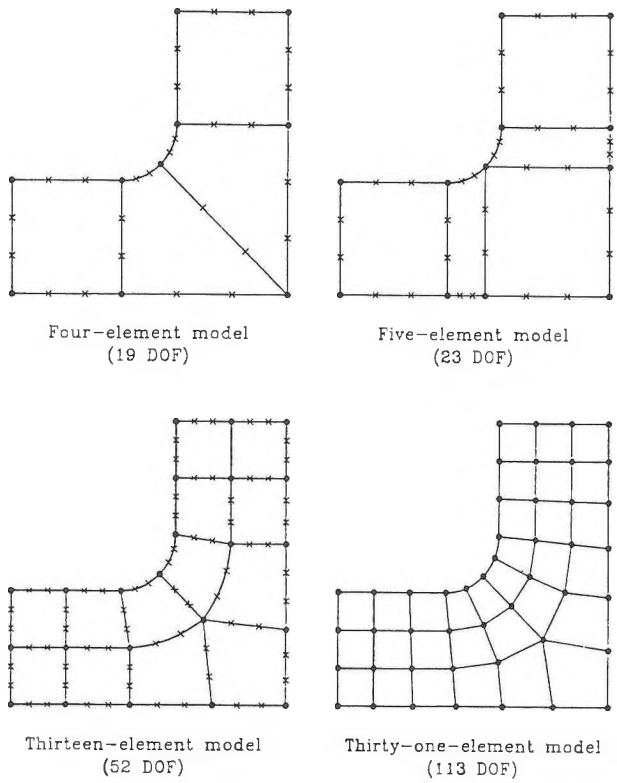

Figure 11: Finite element meshes for a duct bend with an inner corner radius of half the inlet duct width

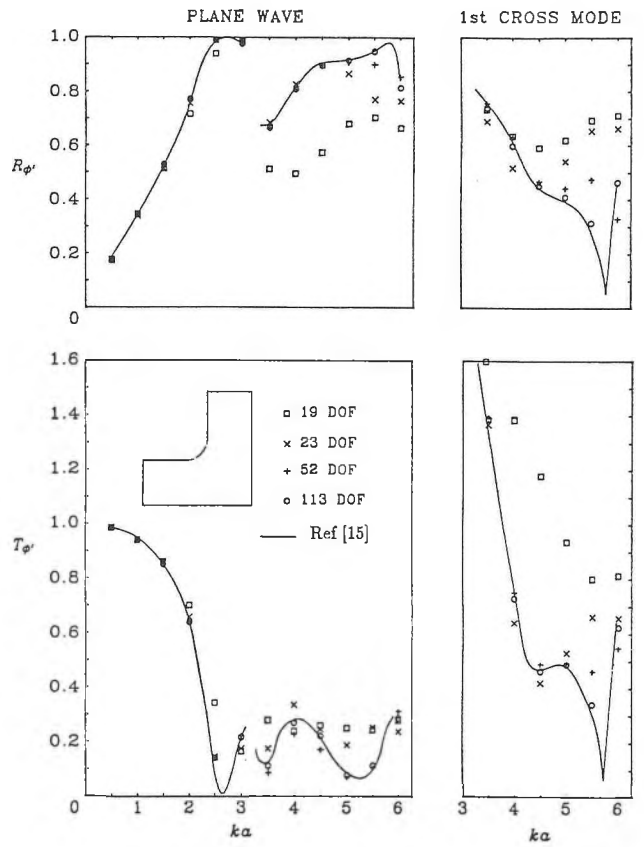

Figure 12: Acoustic velocity potential reflection and transmission coefficients for a bend with inlet and outlet widths a

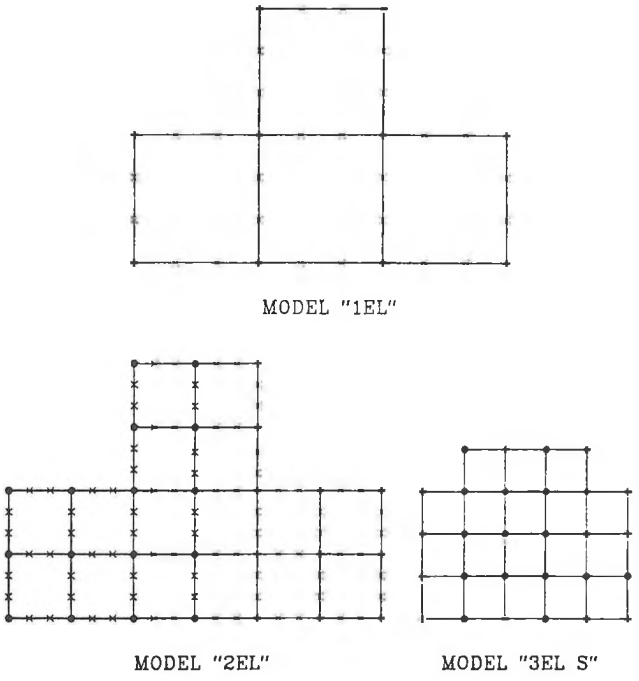

Figure 13: Finite element meshes for a 90° side branch with all connecting ducts of width a

is reflected as a plane wave. Above this cut-on frequency, some acoustic energy is transmitted and reflected both in the first cross mode and the plane wave modes. Cabelli also obtained some results with flow but at Mach numbers too large to be valid with the model developed in the present work.

4.4 Modelling a 90° Side Branch Junction

Compared to the volume of research done on duct bends, there appears to be relatively little research literature concerned with duct junctions. Some solutions with no flow have been obtained for a two-dimensional "T" junction (Miles [24] and von Said [25]) where the incident wave entered the stem of the "T". A 90° side branch was considered by Redmore and Mulholland [26] using a mode coupling theory. This side branch was essentially a "T" junction in which the incident wave entered one arm of the "T". Figure 13 shows element meshes used to model a 90° degree side branch junction which is attached to infinite ducts extending left, right and up from the models shown. Note that with three elements across the duct width, a reduced model with shortened inlet and outlet regions is used due to memory limitations of the computer. This is acceptable for the acoustic problem, since the evanescent and propagating modes are included in the connecting duct boundary conditions, but not acceptable for modelling the flow since longer transition regions are needed for a uniform flow to develop. The duct on the left is taken to contain the incident sound wave and the flow taken as positive when entering this duct and exiting the side branch and the continuing duct to the right.

Before presenting the results for these models, the subject of acoustic intensity and transmitted sound power will be discussed. Flow considerably complicates the definition of acoustic intensity. The definition of acoustic intensity with flow, given by Morfey [23] and also used by Cabelli [15] has been adopted in this work, although as discussed by Eversman [27], this definition does not give correct results with absorptive walls in the presence of flow. The axial acoustic intensity for each propagating mode is integrated over the connecting duct cross-section to give a transmitted sound power for each mode. A reflection coefficient for the reflected m^{th} mode in the duct containing the incident wave can be defined by $R_m = W_m^{\text{refl}}/W^{\text{inc}}$ where W_m^{refl} is the reflected sound power for the m^{th} mode and W^{inc} is the total sound power for the incident modal mixture. Similarly the modal transmission coefficient T_m^i for the m^{th} mode in the i^{th} transmitting duct can be defined by $T_m^i = W_m^i/W^{\text{inc}}$ where W_m^i is the transmitted sound power for the m^{th} mode in the i^{th} transmitting duct. The concept of transmission loss normally used for a single acoustic transmission line is extended to a junction to give the transmission loss TL_m^i for the m^{th} mode in the i^{th} transmitting duct as

$$TL_m^i = -10 \log_{10} T_m^i. \tag{5}$$

A similar equation is used with reflected modes, treating the reflected wave as another transmission path. For lack of a better word this can be called the reflection loss RL_m for the m^{th} mode given by

$$RL_m = -10 \log_{10} R_m. \tag{6}$$

Figure 14 shows the convergence of the finite element models for the 90° side branch with no flow and a plane incident wave. The results are given in terms of transmission loss in decibels. The upper graph shows the reflection loss, RL, for the reflected plane wave and the first cross mode. The lower two graphs show the transmission losses, TL, for the plane wave and the first cross mode in the 90° side branch and in the continuing main duct. Above the cut-on frequency of the first cross mode at $ka = \pi$, most of the sound energy propagates along the continuing straight duct as a plane wave. The results for the model with two elements across the duct width are close to those obtained for the "shortened" model with three elements across the duct width. This would indicate that the models, with only two elements across the duct width, can be used for the problem with flow and give a reasonable approximation of the transmission characteristics over the frequency range considered.

At low frequencies, where the wavelength is large compared to dimensions of the duct junction region, the classical approach to plane wave propagation in pipes can

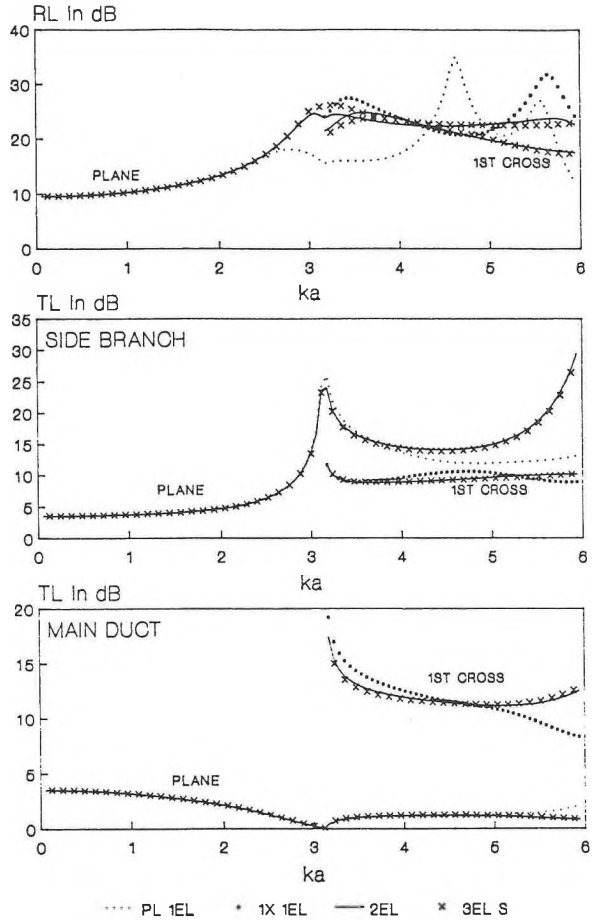

Figure 14: Convergence of FEM models for a 90° side-branch with all ducts of width a and a plane incident wave with no flow

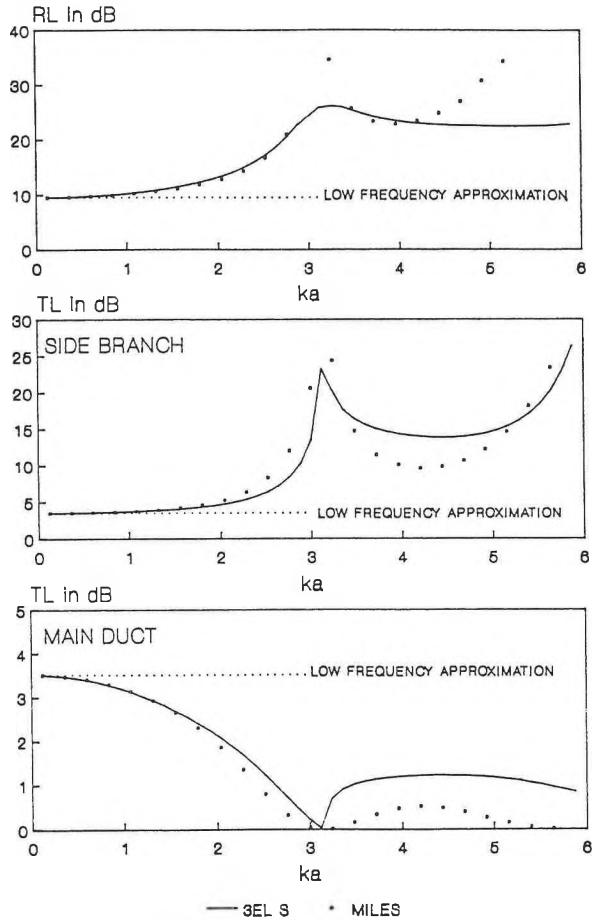

Figure 15: Comparison with other approximate solutions for a 90° side branch with all ducts of width a and a plane incident wave with no flow

be used to derive the transmission characteristics of the junction. This prediction assumes that the acoustic pressure is the same in each duct near the junction and results in transmission and reflection coefficients which are only dependent on the connecting duct cross-sectional areas. An approximate solution was developed by Miles [24] using an electrical circuit analogy which limited his approach to plane waves in connecting ducts and assumed that any higher order modes generated at the junctions decayed over short distances. The finite element prediction of the plane wave reflection and transmission losses with a plane incident wave are compared to the classical low frequency approximation and Miles approximation in Figure 15. For small values of ka the three methods converge to the same value. As the cut-on frequency of the first cross mode is approached one would expect Miles solution to deviate from the true solution. Even above this cut-on frequency Miles results show similar trends to the finite element model results.

Figure 16 shows the change in reflection and transmission loss with flow compared to the no-flow case, for the case of equal flow out the continuing straight duct and side branch, and a plane incident wave. The greatest changes tended to occur near the cross mode cut-on frequencies. At Mach 0.1, the flow generally produced changes in transmission loss of only 1 dB or less. Results were also obtained for the first cross mode incident wave, and for a side branch with one half of the width of the main duct. The ratio of flow out of the continuing duct and side branch was also varied and in all cases the effect of flow on the transmission losses was small. A negative Mach number indicates cases where the flow was taken to be in the opposite direction to the incident wave and transmitted wave propagation.

4.5 Modelling a 45° Side Branch Junction

Figure 17 shows a finite element mesh for a more complex 45 degree side branch junction modelled with only one element across the duct width. The current method is limited to modelling surfaces with more than one element across the connecting duct width only when the interface

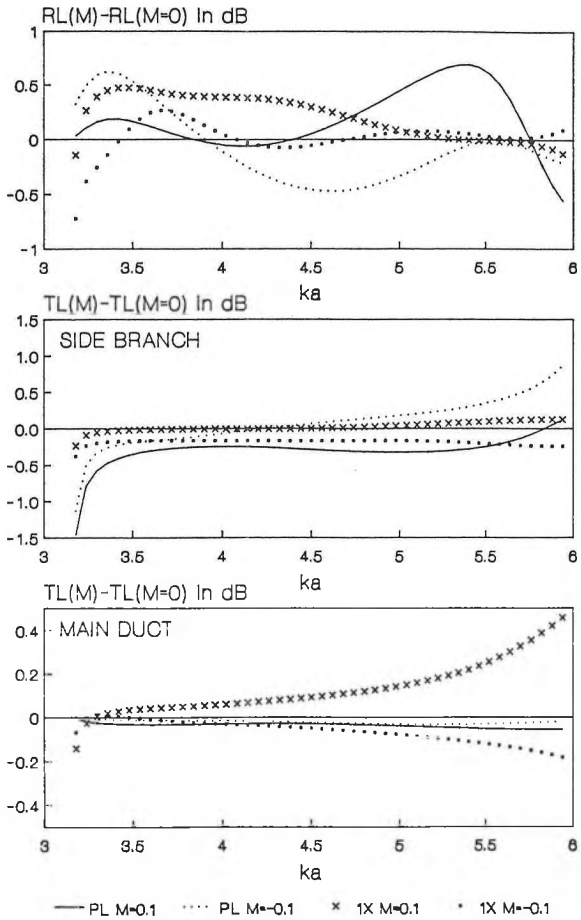

Figure 16: Change in RL and TL with respect to the no-flow case for an equal flow split between the 90° side branch and continuing duct

surfaces are parallel to one of the global axes. When more than one element is used across the duct width, the cross-section acoustic modes are defined in terms of the nodal acoustic velocity potential and tangential derivative nodal quantities at the interface; however, the global model is defined in terms of the derivatives with respect to the global coordinate axes. The conventional isoparametric element does not have this limitation.

The predicted transmission characteristics of this 45 degree side branch model are shown in Figure 18. Note that the cut-on frequency for the first cross mode is different for each duct since each has a different width. The higher frequency results may be inaccurate due to the coarseness of the finite element mesh. The dashed curves show the classical plane wave low frequency approximation. This approximation is commonly used in HVAC acoustic models to predict the sound power split between branches at a junction. The finite element model predictions indicate that even at relatively low frequencies the classical plane wave approximation may not be very realistic.

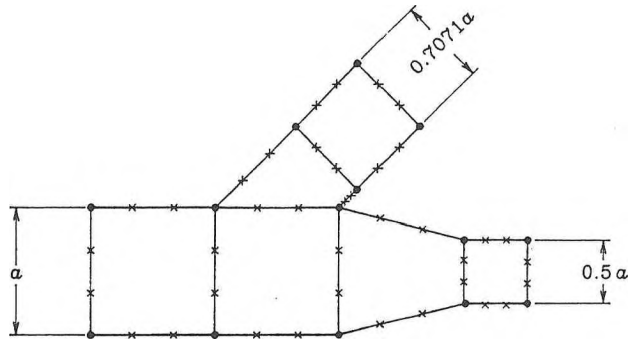

Figure 17: The finite element model of a junction with a 45° side branch

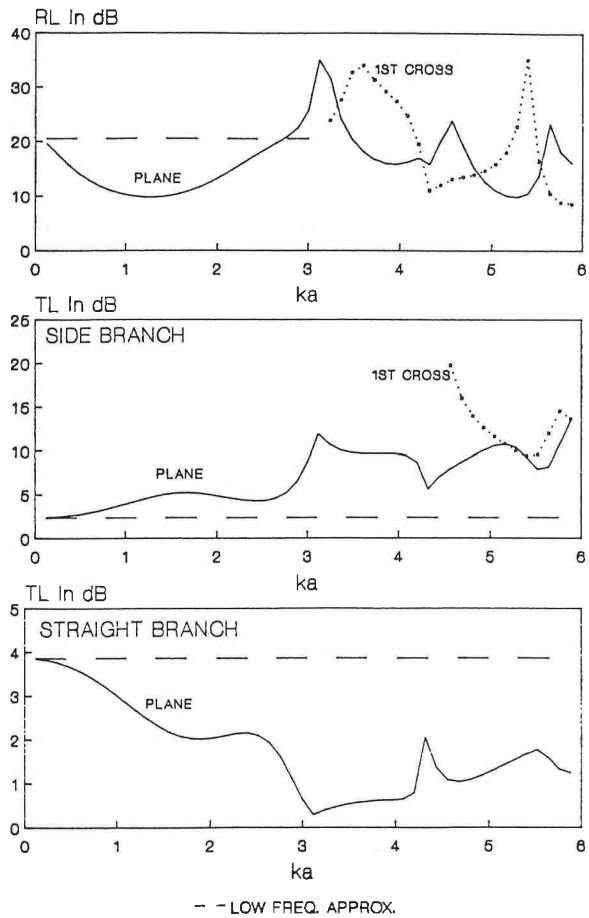

Figure 18: Propagation characteristics of a duct junction with a 45° side branch for a plane wave incident and no flow

5 SUMMARY AND FURTHER WORK

A cubic isoparametric finite element has been developed using Hermite polynomials. The element has been used to model the acoustic propagation characteristics of duct junctions including higher order mode propagation and mean flow effects. The use of this new element has allowed certain problems to be solved on a desktop computer which would have been difficult to solve using the conventional cubic isoparametric element without using a more powerful computer. It was found that flows typical of HVAC systems (Mach 0.1 or less) had only a small effect on the bend and junction transmission losses, changing the component transmission losses by generally less than one decibel with the exception, that near the cross mode cut-on frequencies, changes of a few decibels occurred. Some areas for further research include:

- Investigation of the difference in the behavior observed with the new element compared to the conventional isoparametric element under certain element boundary distortions.
- Confirmation of some of the model results by running larger models on a mainframe computer and also testing three-dimensional junction models with connecting ducts of rectangular and perhaps circular and oval cross-sections. The advantages of the new element over the conventional isoparametric element may not be as great in these cases.
- Modify the existing method to handle duct interfaces at oblique angles.
- Extension of the method of Reference [4] for predictions in duct networks and branched systems to higher frequencies. This could be achieved by including higher order modes in connecting straight duct models in a manner similar to that used in the current work on individual components.
- Include acoustically absorptive linings and flexible duct walls in the prediction method. In these cases the advantage of the new element to reduce the model size by explicitly constraining derivative nodal quantities could not be applied.

ACKNOWLEDGEMENTS

The work presented here has been supported through a grant from the Natural Sciences and Engineering Council of Canada, Grant No.A7431, and through a Killam Scholarship (to D.C.S.).

REFERENCES

[1] Munjal, M.L., *Acoustics of ducts and mufflers with applications to exhaust and ventilation system design*, John Wiley & Sons, New York, 1987.

[2] Eversman, W., "A systematic procedure for the analysis of multiply branched acoustic transmission lines", American Society of Mechanical Engineers Rep. 86-WA/NCA-10, 1986.

[3] Stredulinsky, D.C., Craggs, A., and Faulkner, M.G., "Acoustics of piping and ducts", Canadian Acoustics, Vol. 15, No. 4, 1987, pp. 3-14.

[4] Craggs, A., and Stredulinsky, D.C., "Analysis of acoustic wave transmission in a piping network", Journal of the Acoustical Society of America, Vol. 88, No. 1, 1990, pp. 542-547.

[5] Gladwell, G.M.L., "A finite element method for acoustics", 5^e Congres International D'Acoustique, Paper No. L33, 1965.

[6] Craggs, A., "The transient response of a coupled plate-acoustic system using plate and acoustic finite elements", Journal of Sound and Vibration, Vol. 15, No. 4, 1971, pp. 509-528.

[7] Craggs, A., "The use of simple three dimensional acoustic finite elements for determining the natural modes and frequencies of complex shaped enclosures ", Journal of Sound and Vibration, Vol. 23, No. 3, 1972, pp. 331-339.

[8] Shuku, T., and Ishihara, K., "The analysis of the acoustic field in irregularly shaped rooms by the finite element method", Journal of Sound and Vibration, Vol. 29, No. 1, 1973, pp. 67-76.

[9] Young, C.J., and Crocker, M.J., "Prediction of transmission loss in mufflers by the finite element method", Journal of the Acoustical Society of America, Vol. 57, No. 1, 1975, pp. 144-148.

[10] Craggs, A., and Stead, G., "Sound transmission between enclosures – A study using plate and acoustic finite elements", Acustica, Vol. 35, No. 2, 1976, pp. 89-98.

[11] Stead, G., *Finite element approach to sound transmission*, M.Sc. Thesis, University of Alberta, 1973.

[12] Craggs, A., "A finite element method for modelling dissipative mufflers with a locally reactive lining", Journal of Sound and Vibration, Vol. 54, No. 2, 1977, pp. 285-296.

[13] Astley, R.J. and Eversman, W., "A finite element method for transmission in non-uniform ducts without flow: Comparison with the method of weighted residuals", Journal of Sound and Vibration, Vol. 57, No. 3, 1978, pp. 367-388.

[14] Astley, R.J. and Eversman, W., "Acoustic transmission in non-uniform ducts with mean flow, Part II: The finite element method", Journal of Sound and Vibration, Vol. 74, No. 1, 1981, pp. 103-121.

[15] Cabelli, A., "The influence of flow on the acoustic characteristics of a duct bend for higher order modes – a numerical study", Journal of Sound and Vibration, Vol. 82, No. 1, 1982, pp. 131-149.

[16] Stredulinsky, D.C., *An isoparametric Hermitian finite element for duct acoustics with flow*, Ph.D. Thesis, University of Alberta, 1990.

[17] Burnett, D.S., *Finite element analysis from concepts to applications*, Addison-Wesley, Reading, Massachusetts, 1987.

[18] Morse, M.., *Vibration and Sound*, American Institute of Physics 1986.

[19] Sigman, R.K., Majjigi, R.K., and Zinn, B.T., "Determination of turbofan inlet acoustics using finite elements", American Institute of Aeronautics and Astronautics Journal, Vol. 16, No. 11, 1978, pp. 1139-1145.

[20] Eversman, W., and Astley, R.J., "Acoustic transmission in non-uniform ducts with mean flow, Part I: The method of weighted residuals", Journal of Sound and Vibration, Vol. 74, No. 1, 1981, pp. 89-101.

[21] Ling, S.F., Hamilton J.F., and Allen J.J., "A two-dimensional isoparametric Galerkin finite element for acoustic-flow problems", Transactions of the ASME, Journal of Mechanical Design, Paper No. 82-DET-97, 1982.

[22] Peat, K.S., "Evaluation of four-pole parameters for ducts with flow by the finite element method", Journal of Sound and Vibration, Vol. 84, No. 3, 1982, pp. 389-395.

[23] Morfey, C.L., "Sound transmission and generation in ducts with flow", Journal of Sound and Vibration, Vol. 14, No. 1, 1971, pp. 37-55.

[24] Miles, J.W., "The diffraction of sound due to right-angled joints in rectangular tubes", Journal of the Acoustical Society of America, Vol. 19, No. 4, 1947, pp. 572-579.

[25] von Said, A., "Theorie der schallausbreitung in kanälen mit rechtwinkligen ecken und verzweigungen", Acustica, Vol. 33, 1975, pp. 203-210.

[26] Redmore, T.L., and Mulholland, K.A., "The application of mode coupling theory to the transmission of sound in a sidebranch of a rectangular duct system", Journal of Sound and Vibration, Vol. 85, No. 3, 1982, pp. 323-331.

[27] Eversman, W., "Acoustic energy in ducts: Further observations", Journal of Sound and Vibration, Vol. 62, No. 4, 1979, pp. 517-532.

Superior Instrumentation for Acoustics and Vibration

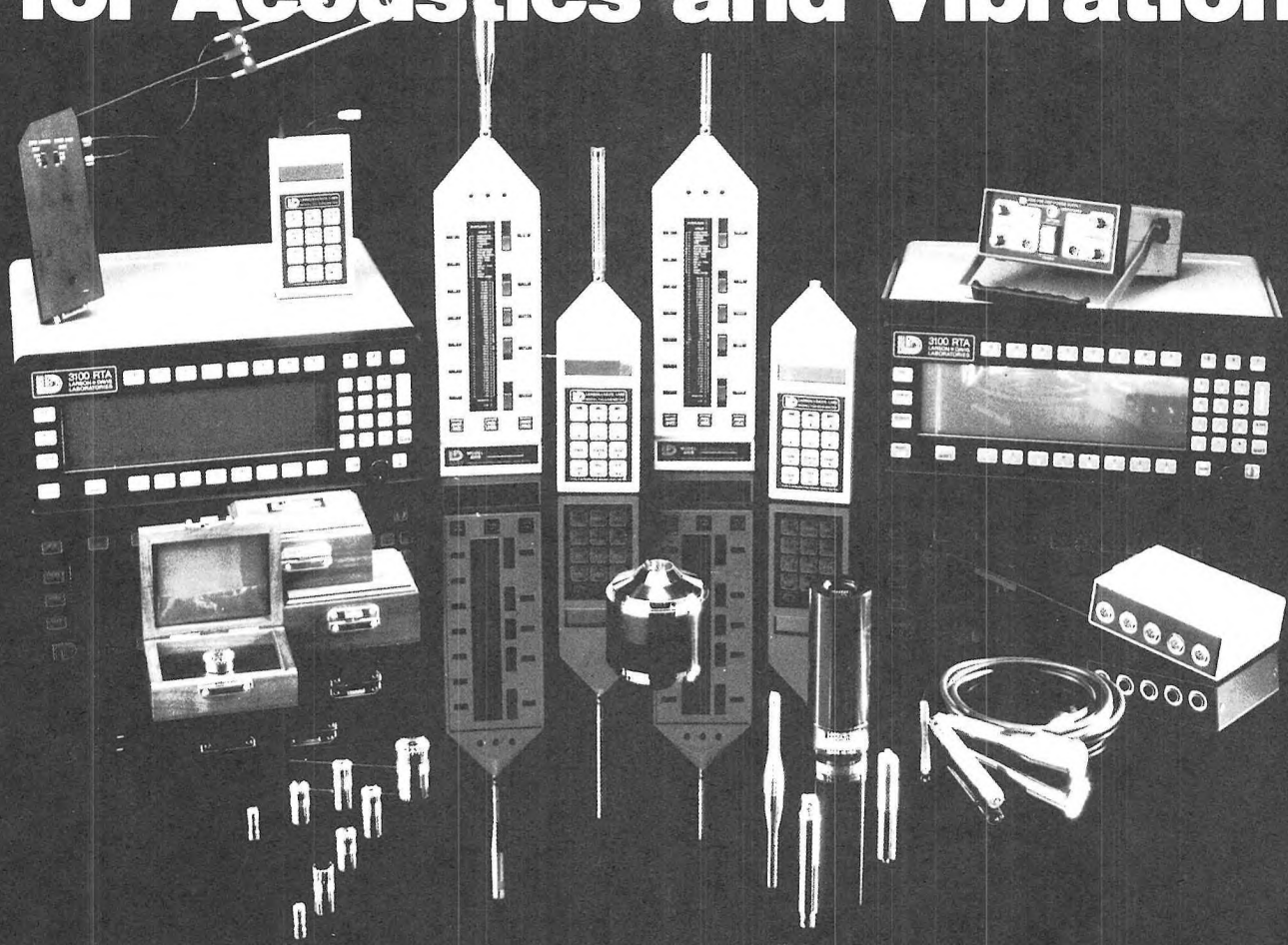

LARSON-DAVIS LABORATORIES

We have become a new technology leader in acoustics and vibration measuring instruments. Our goal is to provide advanced, precise, high-quality products at very reasonable prices. As the result of a substantial ongoing research program, Larson-Davis products provide versatility and automation untouched by *any* competitive offerings. Our growing product family includes:

- Portable multichannel Real-Time analyzers delivering 1/1, 1/3 and 1/12 octave bands to 125 KHz with future plug-in modules for FFT, acoustic intensity, memory expansion, etc.
- Underwater acoustic analysis equipment.
- Precision sound level meters with computer interfaces and automated control of 1/1 and 1/3 octave filters.
- Data logging noise dosimeters and hand-held sound level meters.
- Environmental and industrial noise monitoring systems.
- Building and architectural acoustics analyzers.
- Vibration measuring and monitoring instruments.
- Audiometric calibration instruments for speech and hearing.
- Network airport noise monitoring systems, with management planning software.
- Precision measuring microphones, preamplifiers, power supplies, instrumentation amplifiers, acoustic intensity probes, calibrators and accessories.

For more information contact the factory.

Dalimar Instruments Inc.

89, boul. Don Quichotte
Suite No. 7
Ile Perrot, Qc
J7V 6X2
Tel.: (514) 453-0033
Fax: (514) 453-0554